J IRAN CHEM SOC (2017) 14:2557–2566
DOI 10.1007/s13738-017-1190-1

ORIGINAL PAPER

A chelating polymer resin: synthesis, characterization, adsorption and desorption performance for removal of Hg(II) from aqueous solution

Wangqian Zhuo[1] · Haian Xu[1] · Runsheng Huang[1] · Jie Zhou[1] · Zaizai Tong[1,2,3] · Hujun Xie[2] · Xiang Zhang[3]

Received: 7 January 2017 / Accepted: 28 August 2017 / Published online: 4 September 2017

Abstract A chloromethylated polystyrene-*N*-methyl thiourea chelating resin (DMTUR) was successfully prepared by the reaction of chloromethylated polystyrene beads (PS-Cl) with *N*-methyl thiourea (DMTU). The DMTUR exhibited a high selective adsorption toward Hg(II) in the mixture of different metal ions containing Cu(II), Hg(II), Cd(II), Pb(II), Cr(III) and Ni(II), and the adsorption capacity of Hg(II) approached a maximum with a value of 347 mg/g at pH = 4.0. Moreover, the batch kinetic study showed that the adsorption behavior of Hg(II) presented as a pseudo-second-order manner. And the adsorption isotherms fitted well with Langmuir model, and the maximum uptake of Hg(II) could reach to be 476 mg g^{-1} at 35 °C. The thermodynamics study ensured the adsorption process essentially as favorable and endothermic. Finally, an eluent of 4 M HNO_3 solution could completely remove the adsorbed Hg(II) and the adsorption capacity allowed a high level at least five cycles. As aforementioned appealing properties, the DMTUR with simple technology, high adsorption capacity, significant selectivity and good regenerability may have a potential application in industrial scale as a treatment of enriched Hg(II) in wastewater.

Keywords Hg(II) · Adsorption · Desorption · *N*-Methyl thiourea · Chloromethylated polystyrene beads

Introduction

In past decades, heavy metals such as Hg(II), Zn(II), Pb(II), Ni(II), Cd(II), Cr(III) and Cu(II) ions have received significant concern due to their poor degradation and high bioaccumulation characters even at trace concentrations, which results in ecotoxicological and environmental threats [1–4]. Among them, mercury (Hg) causes particular environmental safety problems due to its extreme toxicity toward aquatic life as well as human bodies [5–10]. However, consideration of a wide use of mercury in industry field, water pollution caused by mercury will be continued to increase. Therefore, detection and removal of mercury metals from wastewater are of great importance, since it can significantly reduce the hazards from perspective of both environment and health.

Various technologies now have been applied for detection and removing mercury from industrial effluents. The main techniques, which have been widely used to remove transition metals from industrial scale, are chemical precipitation [11], ion exchange [12], evaporation, membrane separation [13, 14] and advanced oxidation processes [15]. However, these methods are ineffective or expensive, especially when the transition metal ions are present in the wastewater at low concentrations. By contrast, the utilization of adsorption method to remove metal ions becomes increasingly attractive in treatment of wastewater [16–19]. The distinct

Electronic supplementary material The online version of this article (doi:10.1007/s13738-017-1190-1) contains supplementary material, which is available to authorized users.

✉ Zaizai Tong
tongzz@zstu.edu.cn

[1] Key Laboratory of Advanced Textile Materials and Manufacturing Technology (ATMT), Ministry of Education, Department of Materials Engineering, Zhejiang Sci-Tech University, Hangzhou 310018, People's Republic of China

[2] Engineering Research Center for Eco-Dyeing and Finishing of Textiles, Ministry of Education, Zhejiang Sci-Tech University, Hangzhou 310018, People's Republic of China

[3] Zhejiang Provincial Key Laboratory of Fiber Materials and Manufacturing Technology, Zhejiang Sci-Tech University, Hangzhou 310018, People's Republic of China

advantages of this protocol over aforementioned ones lie in simple operation, good reusability and low cost of the adsorbent [20–22]. For instance, chelating polymers modified by commercially or synthetically functional molecules can interact with metal ions through coordination bond readily in aqueous solution [23–26]. On the other hand, the adsorbed metals can be eluted efficiently by suitable eluent [14, 27, 28]. Therefore, a wide investigation about the properties of various chelating resins has been conducted by many groups [23–28].

With a stable mechanical property, macroporous chloromethylated polystyrene bead (PS-Cl) is an attracting polymeric matrix [29, 30]. The active site of chloro (Cl) in polystyrene can react with different functional molecules, which endows the resin new functions. The inserting chelating ligands usually contain various electron donor atoms such as oxygen, nitrogen and sulfur on the polymer skeleton, and the electronic and steric effects of these atoms allow them to be selective and efficient for the adsorption of specific metal ion [31–33]. For example, resins decorated with functional groups that contain sulfur or nitrogen show excellent performance on selective adsorption of heavy metals [34, 35]. Li [36] prepared a new kind of PS-Cl-based adsorbent owned plenty of sulfamine functional group, and the maximum adsorption capacities for Hg(II) was found to be 222.2 mg/g. Wei [37] synthesized a novel 5-aminopyridine-2-tetrazole-functionalized polystyrene resin. It was found the resin possessed good adsorption capacities for Cu(II), Pb(II) and Hg(II), and the selectivity was different from the commonly used iminodiacetic acid chelating resin. Xiong [38] prepared a novel chloromethylated polystyrene-*g*-2-adenine chelating resin, and the resin exhibited a high selectivity toward Hg(II) in a mixture of different metal ions. Based on the reported paper, the ligands have a crucial effect on the adsorption of metal ions. Therefore, a better understanding of polymer–ligand interactions based on hard–soft acid–base theory could enable us to design excellent chelating polymer with high performance.

Inspired by these studies, herein, we proposed the synthesis of a chelating resin (DMTUR), which was prepared from the reaction of PS-Cl and *N*-methyl thiourea [39]. The introducing of S and N atoms in the polymer backbone endowed the resins a good affinity with metal ions. It was found that the DMTUR has a high selective adsorption (347 mg/g at pH = 4.0) of Hg(II) from multicomponent solutions with Cu(II), Hg(II), Cd(II), Pb(II), Cr(III) and Ni(II). The adsorption capability for Hg(II) in the aqueous solution was investigated by a series of batch and column experiments. To a better understanding of the adsorption process, the adsorption kinetics, isotherms and the thermodynamic of adsorption of Hg(II) on the synthetic resin were sequentially conducted. The recovery of Hg(II) and reusability of the adsorbents were also investigated as well, and the results showed an eluent of 4 M HNO_3 solution could completely remove the adsorbed Hg(II) and the adsorption capacity allowed a high level at least five cycles. Combined with previous reported paper [29, 30, 32], the DMTUR presented simple technology, high adsorption capacity, significant selectivity and good regenerability. These results could provide an efficient pathway to the removal of Hg(II) from waste solutions, and it may be used as a promising material in the industrial scale from environmental protection point.

Experimental

Materials

Chloromethyl polystyrene beads (PS-Cl) (cross-linked with 8% divinylbenzene, chlorine content 19.2 wt%, specific surface area 43 $m^2\ g^{-1}$, diameter ~300 μm) were provided by Chemical Factory of Nankai University of China. *N*-methyl thiourea was purchased from Sigma-Aldrich. Since the anions in this study have negligible effect on the adsorption behavior of metal ions, we prepared the metal ions of Cu(II), Hg(II), Cd(II), Pb(II), Cr(III) and Ni(II) from $CuCl_2$, $HgCl_2$, $Cd(NO_3)_2$, $Pb(NO_3)_2$, $Cr(NO_3)_3$, $NiSO_4$, respectively. All other reagents and solvents were used without any further purification.

Synthesis of resin

The synthesis of polystyrene-supported *N*-methylthiourea resin (DMTUR) was according to a reported paper [39]. The detail process was described as follows. A 100 mg of PS-Cl beads and 125 mL of anhydrous toluene were added to the flask equipped with a condenser, thermometer and swelling overnight. Then, a certain amount of DMTU and a small amount of metallic sodium were added to the flask under repeatedly flushed with nitrogen. The flask was immersed in an oil bath at a preset temperature under a nitrogen atmosphere with vigorously stirring. After completing the reaction, the resulting resin was washed thoroughly with toluene, deionized water, acetone and ether thrice, respectively. And the obtained resin was dried in a vacuum at 40 °C for another day to ensure the removal of residual solvent. The conversion of the functional group of the resin can be calculated from the nitrogen content with the following equations:

$$F_c = \frac{N_c}{14\,n_c} \times 1000 \tag{1}$$

$$X = \frac{1000\,F_c}{1000\,F_0 - \Delta m\,F_c\,F_0} \times 100\% \tag{2}$$

where F_0 and F_c are the contents of the functional group of polystyrene and the synthesized resin, respectively, X is the functional group conversion (%), Δm is the incremental synthesis reaction resin (g mol^{-1}), n_c is the number of nitrogen atoms of ligand molecules, and N_c is the nitrogen content of the synthesized resin (%).

Characterization

Samples for Fourier transform infrared (FT-IR) spectrometer were first dried under an infrared lamp prior to characterize, and spectra were recorded on a Nicolet 6700 instrument. Thermogravimetric analysis (TGA) of samples was performed on Pyris 1 with a heating ramp of 20 °C min^{-1} up to 1000 °C under nitrogen atmosphere. Morphology for the adsorption behavior of the resin was characterized by scanning electron microscopy (SEM) on a Hitachi S-3000 N instrument. The detailed condition for inductively coupled plasma spectroscopy (ICP) was described as following: power: 1.2 kW, carrier gas flow rate: 0.4 L/min, plasma gas flow rate: 16 L/min, nebulizer gas flow rate: 0.8 L/min, auxiliary gas flow velocity: 1.0 L/min, pre-spray time: 30 s, wash time: 20 s.

Resin adsorption and desorption experiments

Batch adsorption experiments were performed in conical flasks containing 30 mL of adsorption solution and 15.0 mg of dried DMTUR. Adsorption of metal ions from multicomponent solution was studied at various pHs (3.0–6.0) in acetic acid–sodium acetate (HAc–NaAc) buffer solution (0.1 mol/L). For better comparison, the adsorption of unmodified chloromethyl polystyrene beads (PS-Cl) was also conducted.

Adsorption experiments were carried out on a shaker at 100 rpm at constant temperatures (15–35 °C) with a pH of 4.0. The residual concentrations of the metal ions were measured at various time intervals by ICP. The adsorption capacity (Q, mg g^{-1}) and distribution coefficient (D) were calculated as the following formulae:

$$Q = \frac{C_0 - C_e}{W} V \tag{3}$$

$$D = \frac{C_0 - C_e}{WC_e} V \tag{4}$$

where C_0 is the initial concentration in solution (mg mL^{-1}); C_e is the equilibrium concentration in solution (mg mL^{-1}); V is the volume of solution (mL); and W is the resin dry weight (g).

Desorption experiments were carried out followed by the adsorption experiments. The resins after complete adsorption were separated by filtration, and then gently washed with deionized water to remove the unabsorbed Hg(II). Then, the resin was agitated with different eluent solutions under various concentrations at 25 °C for 24 h. Subsequently, the concentration of Hg(II) was analyzed as described aforementioned method. The adsorption–desorption cycle was repeated for five times at the same condition. The desorption ratio (E) was calculated as follows:

$$E(\%) = \frac{C_d V_d}{(C_0 - C_e)V} \times 100\% \tag{5}$$

where C_d is the concentration of the solutes in the desorption solutions, V_d is the volume of the desorption solution, and C_0, C_e and V are the same as aforementioned parameters.

Continuous packed bed studies were performed in a fixed-bed mini glass column (3 mm diameter × 30 cm long) with 100.0 mg of resin. The DMTUR in the column was presoaked for 24 h before the experiment. The Hg(II) solution at a designed concentration and flow rate was passed continuously through the stationary bed of absorbent in downflow mode. The experiment continued until a constant Hg(II) ion concentration was obtained. The column studies were performed at the optimum pH at a constant temperature of 15, 25 and 35 °C representative of environmentally relevant conditions.

Results and discussion

Synthesis of PS-Cl-based *N*-methyl thiourea resin (DMTUR)

Since the reaction solvent, temperature and molar ratio have a crucial effect on the resulting functional resin, the optimal reaction condition which is related to the N content (N%) and functional group conversion has been studied. Different solvents such as toluene, DMF, 1,4-dioxane and water are selected as the solvents, and it reveals that DMF is the best solvent for the reaction, in which the N% is high to 10.5% among the four selected solvents (4.30, 7.29 and 0.42% of N% for toluene, 1,4-dioxane and water, respectively). Similarly, the best conditions for the DMTUR are detected to be 90 °C and 4:1 for the reaction temperature and molar ratio of DMTU/PS-Cl, respectively (Table S1 in the supporting information). Consequently, the N% and the functional group conversion at the best condition is 11.7 and 96.9% for the DMTUR, respectively.

Characterization of DMTUR

In order to confirm the possibility of DMTU bonded to PS-Cl resin, FT-IR has first been conducted as shown in

Fig. 1. For a better comparison, the FT-IR spectra of PS-Cl, DMTU and the mixture of PS-Cl +DMTU are also included in Fig. 1. Generally, significant changes are observed in the IR spectrum of DMTUR compared to that of PS-Cl resin. According to reported paper [21], the peaks at 1264 and 673 cm^{-1} are attributed to characteristic peaks of CH_2–Cl. And these two peaks disappear in the spectrum of DMTUR compared with that in PS-Cl spectrum. By contrast, a newly emerging peak at 1167 cm^{-1} assigned to the cooperation of C=S and C–N stretching vibration is observed in the DMTUR spectrum, implying the successful modification of PS-Cl with DMTU. Moreover, compared with the spectra of DMTUR and the mixture of PS-Cl and DMTU, different spectra are detected, which in turn confirms the chemical modification of the PS-Cl resin with DMTU. Based on the above result, the possibly reaction of PS-Cl and DMTU can be depicted as Scheme 1.

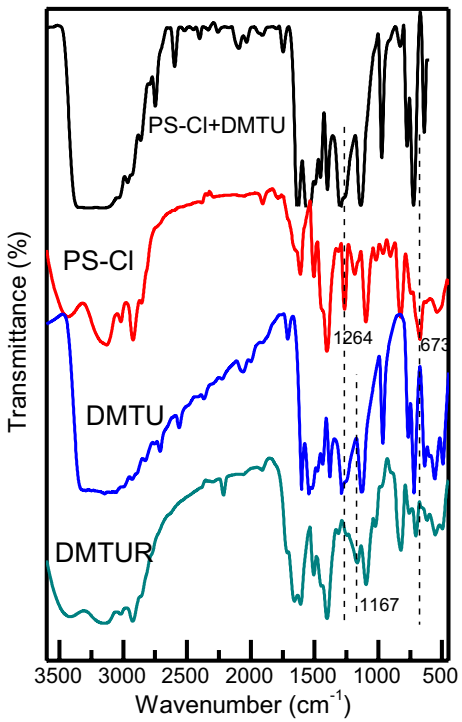

Fig. 1 FT-IR spectra of PS-Cl, DMTU and DMTUR. And the blending of PS-CL and DMTU is also included for comparison. The spectra are normalized and then vertically shifted for better clarification

The thermal properties of PS-Cl, DMTU, DMTUR and mixture of PS-Cl and DMTU have been further characterized by thermogravimetric analysis (TGA) under a nitrogen atmosphere (Fig. 2). It is observed that DMTU begins to decompose at 185 °C, and the decomposition reaches 100% at 320 °C. When it comes to PS-Cl, a two step of decomposition is registered, where two slopes between 200 and 480 °C are present in TGA curve. From 25 to 480 °C, the weight loss of PS-Cl was about 27 wt%, which is quite close to the chloromethyl content (26.7%) in PS-Cl, indicative of the decomposition of C–Cl bond in PS-Cl. In the second weight loss step, about 40 wt% loss from 480 to 1000 °C represents the break of skeleton structure of PS-Cl. As for DMTUR, two stages of weight losses are also observed. The first weight loss ranges from 25 to 355 °C with a loss about 13.6 wt%. Considering the weight content of sulfur in DMTUR (13.4 wt%, which is calculated based on the content of N in DMTUR, Table S1), it can be inferred that the breakdown of C=S bond could account for the weight loss in this step. In the second stage, the decomposition initiates at about 355 °C and a weight loss of 62.5 wt% is detected, which is mainly attributed to the break of skeleton structure of DMTUR. On the other hand, the TGA curve of the blending sample, DMTU + PS-Cl, is quite different from the curve of DMTUR. One can see that the weight loss of DMTU + PS-Cl is more than that of DMTUR at the same temperature, and the total weight loss is also larger than that of DMTU + PS-Cl, which is a consequence of non-chemical bond in DMTUR + PS-Cl.

Selective adsorption behaviors

The selective adsorption property of the DMTUR has been investigated in an aqueous mixture containing Cu(II), Hg(II), Cd(II), Pb(II), Cr(III) and Ni(II) metal ions at different pHs. Figure 3 shows the adsorption behavior with different metals of DMTUR at pH ranging from 3.0 to 6.0. One can see that DMTUR exhibits an obviously high adsorption capacity of

Scheme 1 Proposed synthesis routine of DMTUR

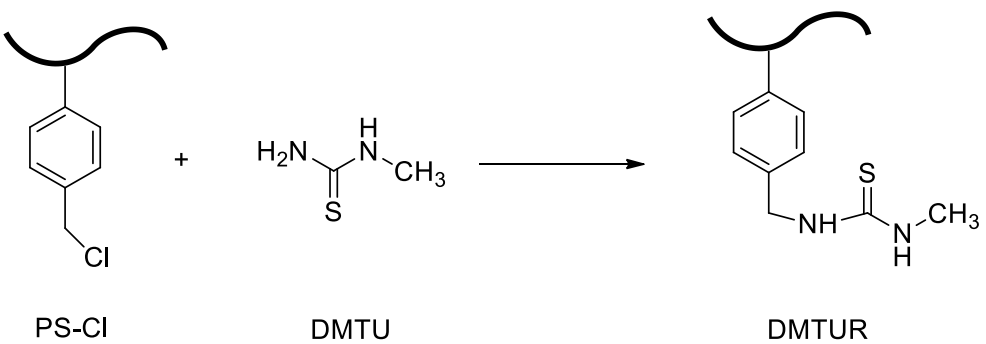

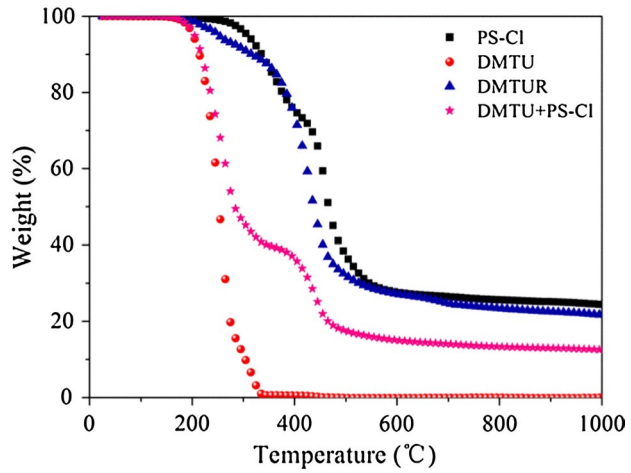

Fig. 2 TGA curves of PS-Cl, DMTU and DMTUR under N_2 atmosphere

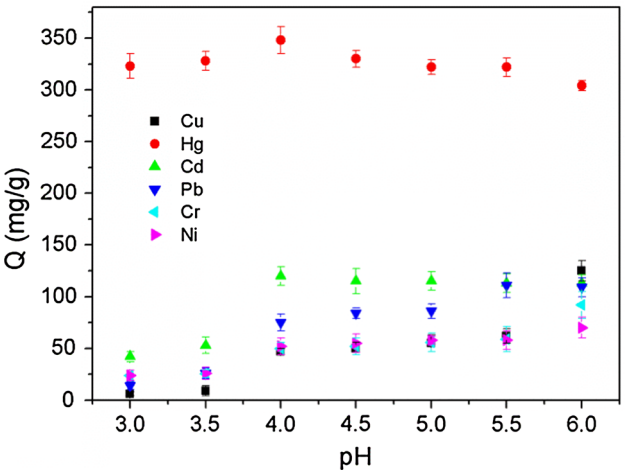

Fig. 3 Adsorption capacities of the DMTUR for Cu(II), Hg(II), Cd(II), Pb(II), Cr(III) and Ni(II) metal ions (resin 15.0 mg, initial metal ion concentration = 10.0 mg/30.0 mL, pH = 3.0–6.0, $T = 298$ K)

Hg(II) than the other metal ions in the studied pH range, which shows that DMTUR exhibits a higher selectivity adsorption for Hg(II). The high adsorption capacity and selectivity for Hg(II) may attribute to the different affinities of DMTUR to Hg(II) and other metal ions [40]. Generally, the –N–H– group contributes to a high adsorption capacity toward Hg(II), while the C=S group is preferred to interact with Hg(II), since soft basic of C=S has a superior affinity toward Hg(II) ions. Moreover, adsorption capacity approaches a maximum with a value of 347 mg/g at pH = 4.0. Further increasing the value of pH, a decreasing adsorption capacity is detected. It is well known that pH can strongly influence the adsorption behavior by alteration of the formation of metal ions and the surface properties of the adsorbents, which further impacts the resulting adsorption amount. When the pH increases, the protonation of N atoms of DMTUR becomes weak and resulting in an enhanced adsorption capacity of DMTUR for Hg(II). However, at very much high pH values, metal hydroxide, such as $Hg(OH)_2$, will be readily formed, which reduces the adsorption ability of DMTUR. Therefore, the optimum pH is set to be 4.0 for DMTUR in this case.

Effect of contact time and temperature

The effect of contact time and temperature on Hg(II) adsorption process was investigated under pH = 4.0 at three indicated temperatures. As shown in Fig. 4, the adsorption capacity of Hg(II) increases rapidly in the first 10 h with a large slope and then levels off to the equilibrium state. The higher metal ion concentration and more active sites available for adsorption of Hg(II) can contribute to a faster adsorption rate in the initial stage. In the late stage of adsorption, the weakened driving force of concentration and higher sterically hindrance result in a low adsorption rate, where the adsorption equilibrium is attained. It is also observed that faster adsorption rate and higher adsorption capacity are obtained at higher temperatures, which is due to the better swelling of the resin and faster diffusion rate of metal ions at higher temperatures. Consequently, the adsorption of Hg(II) onto DMTUR is more effective at higher temperatures.

Adsorption equilibrium isotherms

The adsorption isotherms depict the relationship between the metal ion in solution and that adsorbed on an adsorbent at a desired temperature. The obtained adsorption data are fitted with Langmuir and Freundlich isotherm models,

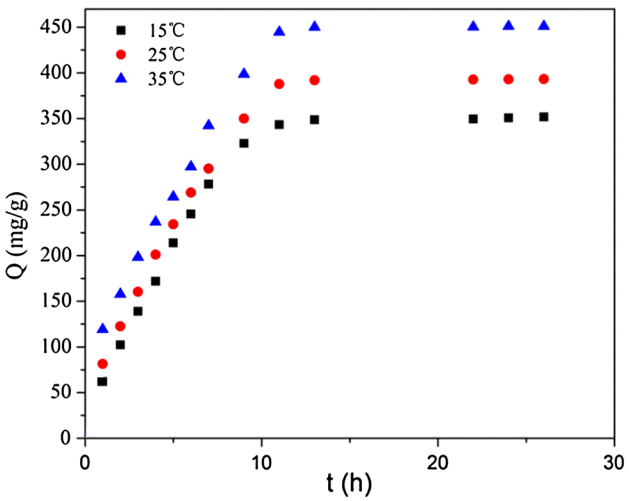

Fig. 4 Adsorption kinetics of Hg(II) at indicated temperatures. (Resin 15.0 mg, $c_{Hg(II)}$ = 10.0 mg/5.0 mL, pH = 4.0)

respectively. The Langmuir isotherm model was developed to describe the adsorption process occurred on the adsorbents with homogeneous and flat surface. This model assumes each adsorptive site can only be occupied once in a one-on-one manner. The linear form of the Langmuir equation is formulated as follows [41]:

$$\frac{C_e}{Q_e} = \frac{C_e}{Q_m} + \frac{1}{Q_m K_L} \tag{6}$$

where Q_e (mg/g) is the equilibrium adsorption capacity, C_e (mg/mL) is the equilibrium concentration, Q_m (mg/g) is the maximum adsorption capacity of Langmuir, K_L (mL/mg) is Langmuir constant related to the energy of adsorption and increases with the increasing strength of the adsorption bond. On the other hand, the Freundlich isotherm model is frequently used to describe the adsorption process occurred on the adsorbents with heterogeneous surfaces. The linear form of the Freundlich model equation is expressed as follows [42]:

$$\log Q_e = \frac{\log C_e}{n} + \log K_F \tag{7}$$

where n is an empirical parameter involving the adsorption intensity, and K_F is roughly an indicator of the adsorption capacity. The fitting figures of above two models are shown in Figs. S1 and S2 in the supporting information, and the fitting parameters obtained from above two isothermal adsorption models are concluded in Table 1. One can see that the adsorption behavior is preferred to present in a Langmuir model manner, since the value of R^2 is evidently larger than that calculated from Freundlich model. This demonstrates that the adsorption of Hg(II) on DMTUR is a monolayer type where the interactions between adsorbed molecules are negligible. On the other hand, the R^2s in Langmuir model are relatively poor, which indicates the real adsorption behavior is much more complicated than simply described Langmuir model.

Kinetics of adsorption

Pseudo-first-order and pseudo-second-order kinetic models can be utilized to simulate adsorption data, and thus the adsorption behavior can be further investigated. The formation of two models can be described as following equations [43, 44]:

$$\log(Q_e - Q_t) = \log Q_1 - \frac{k_1 t}{2.303} \tag{8}$$

$$\frac{t}{Q_t} = \frac{1}{k_2 Q_2^2} + \frac{t}{Q_2} \tag{9}$$

where, Q_e and Q_t are the adsorption capacities at equilibrium state and time t (mg/g), respectively. Q_1 and Q_2 represent the adsorption capacities calculated from pseudo-first-order model and pseudo-second-order model (g mg^{-1}). k_1 and k_2 are the rate constants of the pseudo-first-order model (h^{-1}) and the pseudo-second-order model (g mg^{-1} h^{-1}). The kinetic parameters obtained from Eqs. (8)–(9) are summarized in Table 2. It is observed that the value of correlation coefficient, R_2^2 is larger than that of R_1^2, implying the adsorption behavior can be inclined to explain by pseudo-second-order mechanism, which means the chemical adsorption is the rate-controlling step [45]. On the other hand, the R_2^2s in pseudo-second-order kinetic model is relatively poor, which indicates the real kinetic model is much more complicated than simply described pseudo-second-order kinetic model.

Table 1 Isotherm parameters for Hg(II) adsorption by DMTUR are calculated from both Langmuir (Eq. 6) and Freundlich models (Eq. 7)

Temp (°C)	Langmuir model			Freundlich model		
	Q_m (mg/g)	K_L (mL/mg)	R^2	K_F (mg/g)/(mg/mL)$^{1/n}$	n	R^2
15	370 ± 5	193 ± 3	0.9993	383 ± 82	23.1 ± 8.5	0.8755
25	400 ± 4	313 ± 3	0.9997	422 ± 93	29.9 ± 10.2	0.8532
35	476 ± 8	350 ± 7	0.9981	494 ± 98	27.7 ± 9.3	0.8729

Table 2 Kinetic parameters for Hg(II) adsorption by DMTUR are calculated from both pseudo-first-order (Eq. 8) and pseudo-second-order models (Eq. 9)

Temp (°C)	Q_e, exp (mg/g)	Pseudo-first-order			Pseudo-second-order		
		k_1 (h^{-1})	Q_1 (mg/g)	R_1^2	$k_2 \times 10^4$ g/(mg h)	Q_2 (mg/g)	R_2^2
15	352	0.2448 ± 0.0026	443 ± 53	0.955	4.225 ± 0.014	385 ± 27	0.990
25	393	0.2169 ± 0.0021	456 ± 52	0.958	3.903 ± 0.021	455 ± 38	0.981
35	451	0.2022 ± 0.0028	483 ± 54	0.954	4.598 ± 0.025	500 ± 40	0.983

Thermodynamic parameters

The thermodynamic feasibility and the nature of the adsorption process are further investigated by allowing 15 mg DMTUR to equilibrate with 30 mL of Hg(II) solutions (10 mg/30 mL) under 15, 25 and 35 °C with an initial solution pH of 4.0. The thermodynamic parameters: Gibbs free energy (ΔG), enthalpy (ΔH) and entropy (ΔS) can be calculated using the following equations [46]:

$$\ln D = -\frac{\Delta H}{RT} + \frac{\Delta S}{R} \tag{10}$$

$$D = \frac{Q_e}{C_e} \tag{11}$$

$$\Delta G = \Delta H - T\Delta S \tag{12}$$

where D is the distribution coefficient, R is the gas constant (8.314 J/(mol K)), and T is the absolute temperature. From the linear fit of ln D versus $1/T$, the values of ΔH and ΔS can be calculated from the slope and intercept of line plot, respectively. And the line fitting data are summarized in Table 3. The positive value of calculated ΔH means that the adsorption of DMTUR adsorbents to Hg(II) is essentially endothermic. On the other hand, the calculated value of ΔS is also positive, showing that the adsorption is an entropy-driven process. The increased randomness at the solid-solution interface of adsorbents may account for positive value of ΔS. Based on the values of ΔH and ΔS, the ΔG at three indicated temperatures can be obtained. One can see that the values of ΔG at three temperatures are all negative, which indicates the spontaneous nature of the adsorption process. Moreover, as the temperature increases, the absolute value of ΔG becomes larger, implying that the adsorption is more favored at higher temperatures.

Table 3 Thermodynamic parameters for Hg(II) adsorption by DMTUR

ΔH (kJ/mol)	ΔS (kJ/(mol K))	ΔG (kJ/mol)		
		15 °C	25 °C	35 °C
32.4 ± 2.5	0.1817 ± 0.0108	−19.93	−21.75	−23.57

Desorption and regeneration studies

From above result, it can be concluded that the chemically adsorbed Hg(II) on DMTUR is rather robust. Therefore, development of a facile approach to desorption and regeneration of metal from the resin is highly desirable. Desorption of the adsorbed Hg(II) from DMTUR-Hg resin was investigated by the batch method using HCl, HNO_3 and HCl–thiourea solutions with different concentrations. The characterized values of desorption efficiency are listed in Table 4. It is shown that the desorption efficiency is largely dependent on the eluent solution, and the adsorbed Hg(II) can be completely desorbed by 4 mol/L HNO_3 solution (100%). To determine the reusability of the DMTUR, consecutive adsorption–desorption cycles were conducted using the same beads. The desorption efficiencies of five adsorption–desorption cycles are presented in Fig. 5. It can be seen that adsorption capacity is still maintained at 95.5% even after five cycles, which infers that DMTUR could be repeatedly used to remove Hg(II) from aqueous solution. And it may be considered as an appealing resin for removal of Hg(II) in waste solutions in industry scale.

Dynamic adsorption and desorption

Batch experimental data are usually difficult to apply to fixed-bed adsorption because of the inaccurate data produced by the isotherms for a dynamically operated column. However, fixed-bed column operation provides more efficient utilization of the adsorptive capacity than the batch process. The breakthrough curves at various conditions are

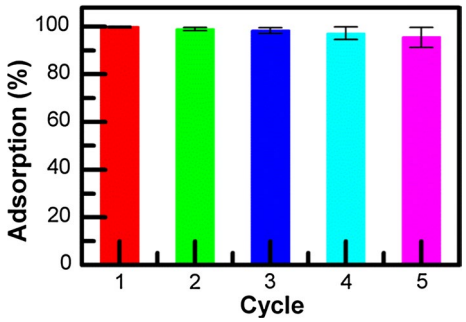

Fig. 5 The adsorption percentage of DMTUR in different cycles. Here, the desorption solution is 4 mol/L HNO_3 and the adsorption solution is 0.1 mol/L HAc–NaAc buffer solution

Table 4 Desorption of DMTUR-Hg(II) by different eluent solutions in various concentrations

Desorption agent	2 M HCL	3 M HCL	4 M HCL	2 M HNO_3	3 M HNO_3	4 M HNO_3	0.5 M HCl + 2.5% thiourea	1 M HCl + 2.5% thiourea
Efficiency	81.0	77.6	85.5	77.2	87.3	100.1	81.1	70.0

presented in Fig. 6. It can be seen that with increasing the initial concentration of metal ion, the breakthrough curve shows a large slope compared with that of low concentration. Meanwhile, fast adsorption rate is observed at a high flow rate of metal ion.

Breakthrough analysis is one of the powerful tools to investigate the efficiency in adsorption columns. The total adsorbed Hg(II) (Q, mg/g) in the column for a given concentration and flow rate can be calculated from following equation [47]:

$$Q = \int_0^v \frac{C_0 - C_e}{m} \mathrm{d}v \tag{13}$$

where C_0 and C_e are metal ion concentrations in the influent and effluent, respectively, m is the mass of the sorbent loaded in the column, and V is the volume of metal solution passed through the column. Designing a column sorption process usually requires prediction of a breakthrough curve or concentration–time profile for the effluent. The maximum adsorption capacity of a sorbent is also taken into consideration. Generally, matching the Thomas model can realize the above requirements, and its form can be described as following forms [48]:

$$\frac{C_e}{C_0} = \frac{1}{1 + \exp[K_T(Qm - C_0)/\theta]} \tag{14}$$

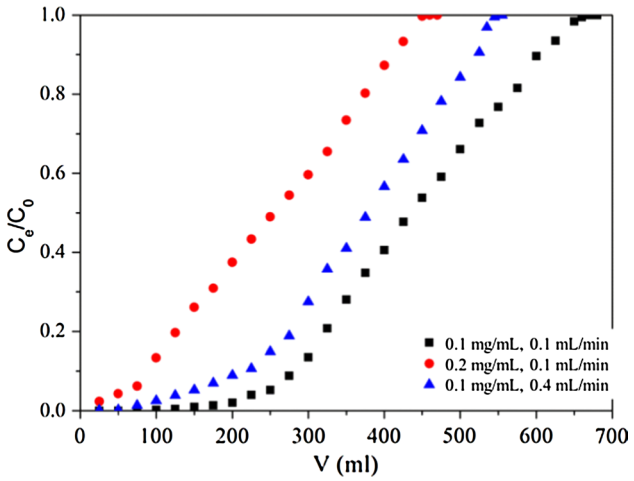

Fig. 6 Breakthrough curves for Hg(II) adsorption in different initial concentrations by DMTUR at different flow rate. (resin 100.0 mg, pH 4.0, $C_0 = 0.20$ mg/mL)

where K_T is the Thomas rate constant (mL/(min mg)), θ is the volumetric flow rate (mL/min), and m is the mass of the resin (g). The linear form of Thomas model can be translated as following:

$$\ln\left(\frac{C_0}{C_e} - 1\right) = \frac{K_T Q m}{\theta} - \frac{K_T C_0}{\theta} V \tag{15}$$

from a linear plot of $\ln[(C_0/C_e) - 1]$ versus V, the K_T and Q can be obtained. And the calculated values at various conditions are summarized in Table 5. One can see the adsorption data are well fitted with Thomas model (a high values of R^2), which demonstrates the validity of applying the Thomas model for the design and simulation of column adsorption. Moreover, the calculated Q is well consistent with the experimental Q_{exp}, indicating that the mechanism of dynamic adsorption process is in accordant with Thomas model. Compared with static adsorption, dynamic adsorption presents a high Q_{exp}. This is due to the constant concentration of Hg(II) in dynamic adsorption, while the concentration of Hg(II) is gradually decreased as the Hg(II) adsorbed to the DMTUR.

Dynamic desorption curve

To study the dynamic desorption of Hg(II) from DMTUR, the 4 M HNO_3 eluent has been employed. The desorption data are plotted with the effluent concentration (C_e) versus elution volume (V) from the column at a flow rate of 0.1 mL/min. As shown in Fig. 7, the complete desorption takes 30 mL of eluent, since after $V = 30$ mL, the C_e is almost 0. Therefore, the 4 M HNO_3 eluent can remove Hg(II) readily from the DMTUR.

Data on the adsorption capacity and desorption ratio of Hg(II) by the recent reported adsorbents were also listed in Table 6. Though some materials exhibit a higher adsorption capacity of Hg(II), the DMTUR with a good overall property (a high adsorption capacity and a 100% desorption ratio) used for Hg(II) removal is still very attractive.

Structure and morphology analysis before and after adsorption

To confirm the structural change before and after adsorption of Hg(II) in DMTUR, FT-IR and TGA of DMTUR-Hg(II) have been conducted as shown in Fig. 8. One can see that the stretching vibration of C–N is located at 1164 cm^{-1}

Table 5 Thomas adsorption model parameters of Hg(II) by DMTUR

C_0 (mg/mL)	θ (mL/min)	K_T (mL/min mg)	Q (mg/g)	Q_{exp} (mg/g)	R^2
0.1	0.1	0.0064	418 ± 18	425	0.9790
0.1	0.4	0.0208	380 ± 8	358	0.9948
0.2	0.1	0.0033	564 ± 13	477	0.9848

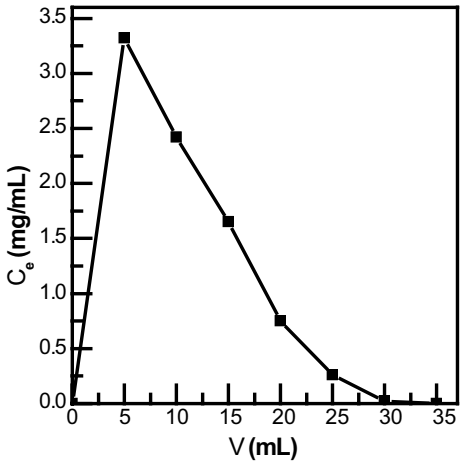

Fig. 7 Dynamic desorption curve of DMTUR-Hg(II) at a flow rate of 0.1 mL/min. The desorption solution is 4 M HNO_3, and the concentration of Hg(II) is 2.0 mg/mL

in DMTUR (Fig. 8a). By contrast, in the DMTUR-Hg(II) spectrum, the stretching vibration of C–N is shifted to 1233 cm^{-1}. The large shift wavenumber of C–N can be attributed to the coordination interaction between N atom in the DMTUR and Hg(II). Moreover, two peaks located at 1610 and 1658 cm^{-1} that belong to C=C bond in the benzene of DMTUR are converted to one peak (1611 cm^{-1}) in the DMTUR-Hg(II) spectrum. This may also be attributed to a strong chemical bond between N atom and Hg(II). The TGA curves for DMTUR before and after adsorption of Hg(II) are shown in Fig. 8b. The decomposition temperature of DMTUR initiates at 195 °C, while after adsorbed Hg(II), the decomposition temperature shifts to 125 °C, indicating that the thermal property of DMTUR-Hg is reduced. Furthermore, the decomposition rate of DMTUR-Hg around 125–325 °C is faster than that of DMTUR. By contrast, the tendency becomes similar when the temperature is above 600 °C. The TGA result illustrates adsorption–desorption of DMTUR can be operated below the temperature of 125 °C. Moreover, we also examined the morphological change

Table 6 Adsorption capacities (Hg^{2+}) of different adsorbents

Adsorbents	Conditions pH/dosage/C[a)]	Adsorption capacities (mg/g)	Desorption ratio	Refs.
2-(Chloromethyl) benzimidazole modified chitosan	4.5/15/(10/30)	258	100	[9]
2-Aminothiazol modified polyacrylonitrile	6.5/15/(10/30)	455	100	[10]
Chitosan-poly(vinyl alcohol)	5.85/50/2.2	586	47	[49]
LPSSF modified Na-montmorillonite clays	5.0/50/0.1	49	80	[50]
Triethylenetetramine bis (methylene phosphonic acid) modified silica gel	5.0/20/0.5	303	–	[51]
DMTUR	4.0/15/(10/30)	476	100	This work

[a] pH value; dosage: weight of resin (mg); C: initial metal ion concentration (mg/mL)

The pH was controlled by the HAc–NaAc buffer solution

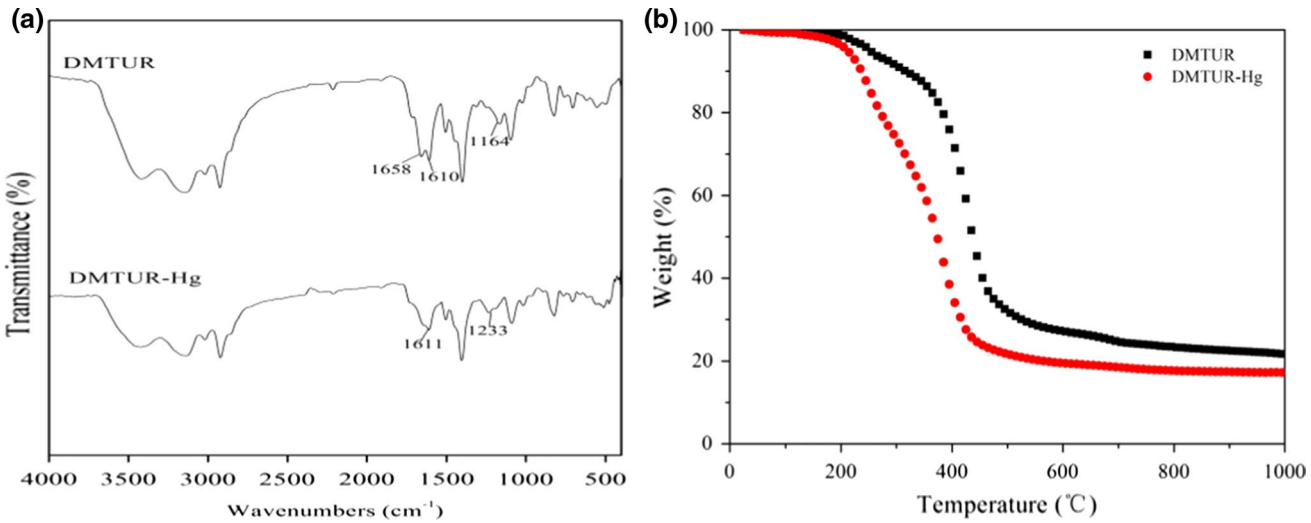

Fig. 8 FT-IR spectra **a** and TGA curves **b** of DMTUR before and after adsorption of Hg(II), and the loading level of Hg(II) is 347 mg/g

before and after adsorption of Hg(II). Figure S3 shows the SEM morphologies of DMTUR and Hg(II)-loaded DMTUR. The surface of synthesized resin is flat and smooth. By contrast, the smooth surface of DMTUR turns coarser with granular flake after adsorbed with Hg(II), which indicates the presence of Hg(II) on the surface of DMTUR.

Conclusions

A chelating polymer-based resin, DMTUR, was successfully synthesized by grafting *N*-methyl thiourea on the surface of PS-Cl beads. The obtained resin presented an excellent selective adsorption ability toward Hg(II) in the mixed metal solutions, and the adsorption capacity of Hg(II) approached a maximum with a value of 347 mg/g at pH = 4.0. Moreover, the adsorption kinetics followed well with pseudo-second-order model, suggesting that chemisorption should be the rate-controlling step. Well-fitted Langmuir isotherm indicated that the adsorption mechanism exhibited a monolayer adsorption manner. Thermodynamic analysis suggested that the uptake of Hg(II) to the adsorbent was spontaneous in nature. Complete desorption of Hg(II) was achieved by using 4 M HNO_3 solution, and the regenerated adsorbents could be reused for many times with high performance. As aforementioned appealing properties, the DMTUR with simple technology, high adsorption capacity, significant selectivity and good regenerability may have a potential application in industrial scale as a treatment of enriched Hg(II) in wastewater.

Acknowledgements This work is supported by Zhejiang Provincial Key Laboratory of Fiber Materials and Manufacturing Technology (No. 2015002), and Zhejiang Provincial Top Key Academic Discipline of Chemical Engineering and Technology, Zhejiang Sci-Tech University (No. YR2015002).

References

1. R.A.K. Rao, S. Ikram, J. Ahmad, J. Iran. Chem. Soc. **8**, 931 (2011)
2. S. Tangestaninejad, I. Mohammadpoor-Baltork, M. Moghadam, V. Mirkhani, M.R. Iravani, V. Ahmadi, J. Iran. Chem. Soc. **9**, 61 (2012)
3. Y.Q. Liu, Y.G. Liu, X.J. Hu, Y.M. Guo, Trans. Nonferr. Met. Soc. China **23**, 3095 (2013)
4. M. Lu, Y.M. Zhang, X.H. Guan, X.H. Xu, T.T. Gao, Trans. Nonferr. Met. Soc. China **24**, 1912 (2014)
5. X.J. Ma, Y.F. Li, Z.F. Ye, L.Q. Yang, L.C. Zhou, L.Y. Wang, J. Hazard. Mater. **185**, 1348 (2011)
6. J.H. Li, W.H. Lu, J.P. Ma, L.X. Chen, Microchim. Acta **175**, 301 (2011)
7. Z.F. Liu, Z.L. Zhu, H.T. Zheng, S.H. Hu, Anal. Chem. **84**, 10170 (2012)
8. H. Javadian, M. Ghaemy, M. Taghavi, J. Mater. Sci. **49**, 232 (2013)
9. C.H. Xiong, L.L. Pi, X.Y. Chen, L.Q. Yang, C.A. Ma, X.M. Zheng, Carbohydr. Polym. **98**, 1222 (2013)
10. C.H. Xiong, Q. Jia, X.Y. Chen, G.T. Wang, C.P. Yao, Ind. Eng. Chem. Res. **52**, 4978 (2013)
11. M.A. Tofighy, T. Mohammadi, J. Hazard. Mater. **185**, 140 (2011)
12. H. Deligöz, E. Erdem, J. Hazard. Mater. **154**, 29 (2008)
13. H. Bessbousse, T. Rhlalou, J.F. Verchère, L. Lebrun, J. Membr. Sci. **307**, 249 (2008)
14. S.A. Ali, I.W. Kazi, N. Ullah, Ind. Eng. Chem. Res. **54**, 9689 (2015)
15. T.A. Kurniawan, G.Y.S. Chan, W.H. Lo, S. Babel, Chem. Eng. J. **118**, 83 (2006)
16. C.H. Xiong, C.P. Yao, X.M. Wu, Hydrometallurgy **90**, 221 (2008)
17. C.H. Xiong, X.Y. Chen, C.P. Yao, J. Rare Earth **29**, 979 (2011)
18. Z. Zhang, J.H. Li, X.L. Song, J.P. Ma, L.X. Chen, RSC Adv. **4**, 46444 (2014)
19. M. Cegłowski, G. Schroeder, Chem. Eng. J. **259**, 885 (2015)
20. C.H. Xiong, X.Y. Chen, X.Z. Liu, Chem. Eng. J. **203**, 115 (2012)
21. C.H. Xiong, Y.Q. Zheng, Y.J. Feng, C.P. Yao, C.A. Ma, X.M. Zheng, J.X. Jiang, J. Mater. Chem. A **2**, 5379 (2014)
22. M.L. Rahman, S.M. Sarkar, M.M. Yusoff, M.H. Abdullah, RSC Adv. **6**, 745 (2016)
23. C.H. Xiong, C.P. Yao, L. Wang, J.J. Ke, Hydrometallurgy **98**, 318 (2009)
24. L.J. Li, F.Q. Liu, X.S. Jing, P.P. Ling, A.M. Li, Water Res. **45**, 1177 (2011)
25. M. Rajiv Gandhi, N. Viswanathan, S. Meenakshi, Ind. Eng. Chem. Res. **51**, 5677 (2012)
26. J.N. Wang, C. Cheng, X. Yang, C. Chen, A.M. Li, Ind. Eng. Chem. Res. **52**, 4072 (2013)
27. C.H. Xiong, Z.W. Zheng, J. Rare Earth **28**, 862 (2010)
28. M. Monier, D.A. Abdel-Latif, Chem. Eng. J. **221**, 452 (2013)
29. C.H. Xiong, X.Y. Chen, C.P. Yao, Curr. Org. Chem. **16**, 1942 (2012)
30. C.H. Xiong, C.P. Yao, Chem. Eng. J. **155**, 844 (2009)
31. M.F. Bari, M.S. Hossain, I.M. Mujtaba, S.B. Jamaluddin, K. Hussin, Hydrometallurgy **95**, 308 (2009)
32. C.H. Xiong, S.G. Zhou, X.Z. Liu, Q. Jia, C.A. Ma, X.M. Zheng, Ind. Eng. Chem. Res. **53**, 2441 (2014)
33. C.X. Li, J.T. Dou, J.J. Cao, Z.Q. Li, W.K. Chen, Q.Z. Zhu, C.F. Zhu, J. Organomet. Chem. **727**, 37 (2013)
34. Y. Hamabe, Y. Hirashima, J. Izumi, K. Yamabe, A. Jyo, React. Funct. Polym. **69**, 828 (2009)
35. P. Nutthanara, W. Ngeontae, A. Imyim, T. Kreethadumrongdat, J. Appl. Polym. Sci. **116**, 801 (2010)
36. Y. Qi, X. Jin, C. Yu, Y. Wang, L. Yang, Y. Li, Chem. Eng. J. **233**, 315 (2013)
37. Y. Zhang, Y. Chen, C. Wang, Y. Wei, J. Hazard. Mater. **276**, 129 (2014)
38. S. Li, Y. Feng, L. Fang, X. Zheng, D. Chen, L. Yao, C. Xiong, Can. J. Chem. **94**, 751 (2016)
39. A.C. Spivey, C.G. Manas, I. Mann, Chem. Commun. **41**, 4426 (2005)
40. X. Dong, L.Q. Ma, Y. Zhu, Y. Li, B. Gu, Environ. Sci. Technol. **47**, 12156 (2013)
41. I. Langmuir, J. Am. Chem. Soc. **40**, 1361 (1918)
42. H.M.F. Freundlich, Z. Phys. Chem. **57**, 385 (1906)
43. Y.S. Ho, Water Res. **37**, 2323 (2003)
44. Y.S. Ho, G. McKay, Process Saf. Environ. Prot. **76**, 332 (1998)
45. M. Monier, D.A. Abdel-Latif, J. Hazard. Mater. **250–251**, 122 (2013)
46. N. Ünlü, M. Ersoz, J. Hazard. Mater. **136**, 272 (2006)
47. M. Tabakci, M. Yilmaz, J. Hazard. Mater. **151**, 331 (2008)
48. T. Mathialagan, T. Viraraghavan, J. Hazard. Mater. **94**, 291 (2002)
49. X.H. Wang, W.Y. Deng, Y.Y. Xie, C.Y. Wang, Chem. Eng. J. **228**, 232 (2013)
50. Z. Zhu, C. Gao, Y.L. Wu, L.F. Sun, X.L. Huang, W. Ran, Q.R. Shen, Bioresour. Technol. **147**, 378 (2013)
51. Z.D. Wang, P. Yin, Z. Wang, R.J. Qu, X.G. Liu, Ind. Eng. Chem. Res. **51**, 8598 (2012)